JOC Article
pubs.acs.org/joc

Induced Folding by Chiral Nonplanar Aromatics

Sri Kamesh Narasimhan, Deborah J. Kerwood, Lei Wu, Jun Li, Rosina Lombardi, Teresa B. Freedman,* and Yan-Yeung Luk*

Department of Chemistry, Syracuse University, Syracuse, New York 13244

tbfreedm@syr.edu; yluk@syr.edu

Received June 17, 2009

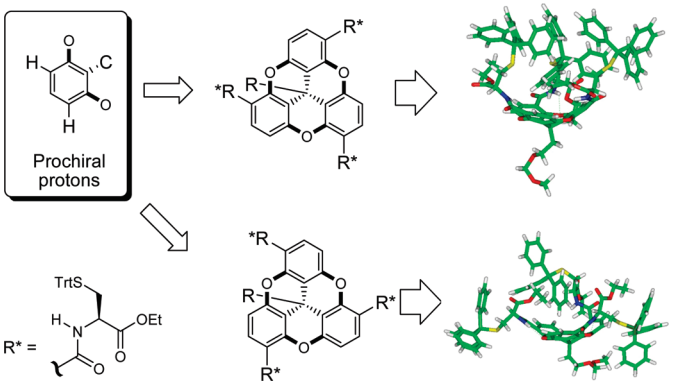

We report a structural motif based on a C_3-symmetric bowl-shaped core, on which three substituted amino acids on the periphery adopt either a folded or a spread-out conformation. This class of chiral folded structures is achieved by controlling the reactivity of the stereogenic protons on the nonplanar aromatic rings of trioxatricornan to afford predominantly C_3-symmetric isomers. Bromination of trioxatricornan afforded a C_1-symmetric and a C_3-symmetric trisubstituted isomer, with the former being the major product as a statistical consequence during the reaction cascade. To obtain the C_3 symmetric isomer as the major product, C−H activation by means of ortho-lithiation with the bulky tert-butyl lithium and tetramethylethylenediamine was followed by a nucleophilic substitution that successfully reversed the statistically controlled regioselectivity. Further derivatization of the trioxatricornan with amino acids or menthol afforded diastereomers that were resolved by preparative chromatography. The absolute configurations of the diastereomers were determined by vibrational circular dichroism (VCD) in combination with density functional theory (DFT) and electronic circular dichroism (ECD). The folding structure of cysteine-derivatized trioxatricornan diastereomers was determined by two-dimensional NMR spectroscopy and molecular dynamics calculation, which revealed that one diastereomer has the amino acids folded toward the cavity of trioxatricornan and the other has a "spread-out" structure.

Introduction

Folding of natural macromolecules is often a consequence of linear polymers that can form helices or sheet-like structures.[1−4] In particular, a recent report described the folding of a peptide containing ten amino acid residues.[5] In this work, we report the design and synthesis of a dissymmetric nonplanar molecular core that induces folding of its three substituents on the periphery. We

*To whom correspondence should be addressed. Phone: (315) 443-7440 (Y.-Y.L.) and (315) 443-1134 (T.B.F.). Fax: (315) 443-4070 (T.B.F.).

(1) Chen, F.; Zhu, N.-Y.; Yang, D. *J. Am. Chem. Soc.* **2004**, *126*, 15980–15981.

(2) Gellman, S. H. *Acc. Chem. Res.* **1998**, *31*, 173–180.

(3) Hecht, S.; Huc, I.; Eds.; *Foldamers: Structure, Properties and Applications*; Wiley-VCH : Weinheim, Germany, 2007.

(4) Hill, D. J.; Mio, M. J.; Prince, R. B.; Hughes, T. S.; Moore, J. S. *Chem. Rev.* **2001**, *101*, 3893–4011.

(5) Honda, S.; Akiba, T.; Kato, Y. S.; Sawada, Y.; Sekijima, M.; Ishimura, M.; Ooishi, A.; Watanabe, H.; Odahara, T.; Harata, K. *J. Am. Chem. Soc.* **2008**, *130*, 15327–15331.

DOI: 10.1021/jo9013047 Published on Web 08/12/2009
© 2009 American Chemical Society

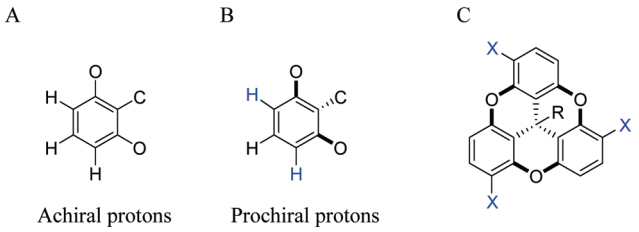

FIGURE 1. Protons are transformed from achiral to prochiral by making a planar (A) aromatic moiety nonplanar (B). Such a nonplanar aromatic moiety can be introduced by a bowl-shaped trioxatricornan (C). Substituting the prochiral protons with a substitutent renders the molecule chiral.

describe the synthesis that reverses the statistically controlled regiochemistry resulting in diastereomers with a C_3-symmetric core. The resolution, absolute configuration determination, and folding characterization for the diastereomers having a C_3-symmetric core are also elucidated.

A wide range of non-natural molecules have been demonstrated to fold into preferred structures among a large ensemble of possible conformations. Examples include β-peptide[2,4,6] and *m*-phenylene ethynylene oligomers.[4,7−9] Other folded structures include synthetic oligomers,[1−4,10−12] synthetic α-peptide sequences,[13−19] artificial proteins,[20−28] nucleic acids,[29−32] and helical polymers.[33−38] Most of these folding molecules involve stereogenic centers on a linear polymer or oligomer. The use of highly symmetric, but chiral moieties to build molecules that fold into preferred conformations has not been extensively studied.[39] Many C_3 symmetric, but achiral molecules have been explored for their utility toward recognition,[40,41] molecular folding,[42] and catalysis.[43,44] To make use of the C_3 symmetry for designing functions, Anslyn and co-workers have built C_{3v} symmetric receptors for facial selectivity[40] and for selective binding of phosphate ions.[41]

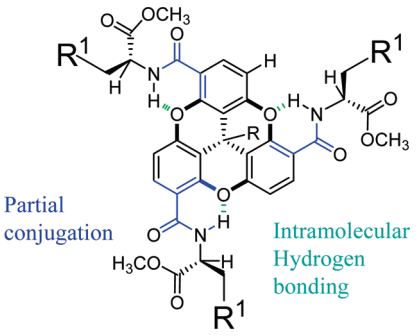

FIGURE 2. Potential intramolecular interactions for trioxatricornan core substituted with three amino acid residues at the C_3-symmetric positions.

We are interested in discovering new folding motifs and self-assembly from non-natural structures,[45] and exploring the biocompatibility and new functions[46] from these unique structures, as well as molecules with exotic symmetries.[47−49] Here, we explore using a chiral C_3-symmetric core[50−55] and intramolecular interactions to induce a folded structure. We reason that while protons on a planar aromatic ring are, in general, not prochiral (Figure 1A), protons on a nonplanar aromatic ring can be prochiral (Figure 1B). To study the effect of the chiral microenvironment of a nonplanar aromatic on molecular conformation and folding, we consider a bowl-shaped core

(6) Petersson, E. J.; Schepartz, A. *J. Am. Chem. Soc.* **2008**, *130*, 821–823.
(7) Elliott, E. L.; Ray, C. R.; Kraft, S.; Atkins, J. R.; Moore, J. S. *J. Org. Chem.* **2006**, *71*, 5282–5290.
(8) Hartley, C. S.; Elliott, E. L.; Moore, J. S. *J. Am. Chem. Soc.* **2007**, *129*, 4512–4513.
(9) Kelley, R. F.; Rybtchinski, B.; Stone, M. T.; Moore, J. S.; Wasielewski, M. R. *J. Am. Chem. Soc.* **2007**, *129*, 4114–4115.
(10) Li, X.; Yang, D. *Chem. Commun.* **2006**, 3367–3379.
(11) Yang, D.; Zhang, D.-W.; Hao, Y.; Wu, Y.-D.; Luo, S.-W.; Zhu, N.-Y. *Angew. Chem., Int. Ed.* **2004**, *43*, 6719–6722.
(12) Horne, W. S.; Gellman, S. H. *Acc. Chem. Res.* **2008**, *41*, 1399–1408.
(13) Balaram, P. *Curr. Opin. Struct. Biol.* **1992**, *2*, 845–851.
(14) Betz, S. F.; Bryson, J. W.; DeGrado, W. F. *Curr. Opin. Struct. Biol.* **1995**, *5*, 457–463.
(15) DeGrado, W. F.; Summa, C. M.; Pavone, V.; Nastri, F.; Lombardi, A. *Annu. Rev. Biochem.* **1999**, *68*, 779–819.
(16) Karle, I. L.; Balaram, P. *Biochemistry* **1990**, *29*, 6747–6756.
(17) Venkatraman, J.; Shankaramma, S. C.; Balaram, P. *Chem. Rev.* **2001**, *101*, 3131–3152.
(18) Singh, Y.; Dolphin, G. T.; Razkin, J.; Dumy, P. *ChemBioChem* **2006**, *7*, 1298–1314.
(19) DeGrado, W. F. *Adv. Protein Chem.* **1988**, *39*, 51–124.
(20) Ansari, A. Z.; Mapp, A. K.; Nguyen, D. H.; Dervan, P. B.; Ptashne, M. *Chem. Biol.* **2001**, *8*, 583–592.
(21) Kirby, A. J. *Angew. Chem., Int. Ed.* **1996**, *35*, 707–724.
(22) Lokey, R. S.; Iverson, B. L. *Nature* **1995**, *375*, 303–305.
(23) Mutter, M. *Angew. Chem.* **1985**, *97*, 639–654.
(24) Nelson, J. C.; Saven, J. G.; Moore, J. S.; Wolynes, P. G. *Science* **1997**, *277*, 1793–1796.
(25) Patch, J. A.; Barron, A. E. *Curr. Opin. Chem. Biol.* **2002**, *6*, 872–877.
(26) Qiu, J. X.; Petersson, E. J.; Matthews, E. E.; Schepartz, A. *J. Am. Chem. Soc.* **2006**, *128*, 11338–11339.
(27) Razeghifard, R.; Wallace, B. B.; Pace, R. J.; Wydrzynski, T. *Curr. Protein Pept. Sci.* **2007**, *8*, 3–18.
(28) Wu, C. W.; Seurynck, S. L.; Lee, K. Y. C.; Barron, A. E. *Chem. Biol.* **2003**, *10*, 1057–1063.
(29) Nielsen, P. E. *Mol. Biotechnol.* **2004**, *26*, 233–248.
(30) Rothemund, P. W. K. *Nature* **2006**, *440*, 297–302.
(31) Chworos, A.; Jaeger, L. *Foldamers* **2007**, 291–329.
(32) LaBean, T. H.; Yan, H.; Kopatsch, J.; Liu, F.; Winfree, E.; Reif, J. H.; Seeman, N. C. *J. Am. Chem. Soc.* **2000**, *122*, 1848–1860.
(33) Amabilino, D. B.; Serrano, J.-L.; Sierra, T.; Veciana, J. *J. Polym. Sci., Part A: Polym. Chem.* **2006**, *44*, 3161–3174.
(34) Green, M. M.; Peterson, N. C.; Sato, T.; Teramoto, A.; Cook, R.; Lifson, S. *Science* **1995**, *268*, 1860–1866.
(35) Maeda, K.; Yashima, E. *Top. Curr. Chem.* **2006**, *265*, 47–88.
(36) Nakano, T.; Okamoto, Y. *Chem. Rev.* **2001**, *101*, 4013–4038.
(37) Nolte, R. J. M. *Chem. Soc. Rev.* **1994**, *23*, 11–19.
(38) Yashima, E.; Maeda, K. *Foldamers* **2007**, 331–366.
(39) Rump, E. T.; Rijkers, D. T. S.; Hilbers, H. W.; de Groot, P. G.; Liskamp, R. M. J. *Chem.—Eur. J.* **2002**, *8*, 4613–4621.
(40) Hennrich, G.; Lynch, V. M.; Anslyn, E. V. *Chem.—Eur. J.* **2002**, *8*, 2274–2278.
(41) Tobey, S. L.; Jones, B. D.; Anslyn, E. V. *J. Am. Chem. Soc.* **2003**, *125*, 4026–4027.
(42) Kwak, J.; De Capua, A.; Locardi, E.; Goodman, M. *J. Am. Chem. Soc.* **2002**, *124*, 14085–14091.
(43) Kemp, D. S.; Petrakis, K. S. *J. Org. Chem.* **1981**, *46*, 5140–5143.
(44) Das, S.; Incarvito, C. D.; Crabtree, R. H.; Brudvig, G. W. *Science* **2006**, *312*, 1941–1943.
(45) Han, Y.; Cheng, K.; Simon, K. A.; Lan, Y.; Sejwal, P.; Luk, Y.-Y. *J. Am. Chem. Soc.* **2006**, *128*, 13913–13920.
(46) Sejwal, P.; Han, Y.; Shah, A.; Luk, Y.-Y. *Org. Lett.* **2007**, *9*, 4897–4900.
(47) Narasimhan, S. K.; Lu, X.; Luk, Y.-Y. *Chirality* **2008**, *20*, 878–884.
(48) Stang, P. J.; Olenyuk, B. *Acc. Chem. Res.* **1997**, *30*, 502–518.
(49) Seidel, S. R.; Stang, P. J. *Acc. Chem. Res.* **2002**, *35*, 972–983.
(50) Canary, J. W.; Allen, C. S.; Castagnetto, J. M.; Wang, Y. *J. Am. Chem. Soc.* **1995**, *117*, 8484–8485.
(51) Gibson, S. E.; Castaldi, M. P. *Angew. Chem., Int. Ed.* **2006**, *45*, 4718–4720.
(52) Moberg, C. *Angew. Chem., Int. Ed.* **1998**, *37*, 248–268.
(53) Bolm, C.; Meyer, N.; Raabe, G.; Weyhermuller, T.; Bothe, E. *Chem. Commun.* **2000**, 2435–2436.
(54) Bolm, C.; Davis, W. M.; Halterman, R. L.; Sharpless, K. B. *Angew. Chem.* **1988**, *100*, 882–883.
(55) Bolm, C.; Sharpless, K. B. *Tetrahedron Lett.* **1988**, *29*, 5101–5104.

SCHEME 1

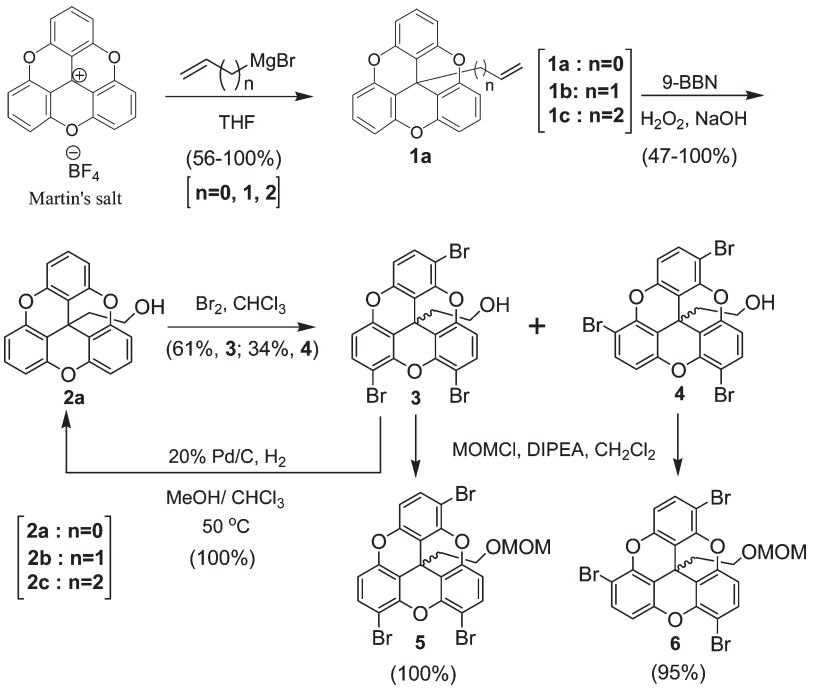

structure of trioxatricornan (Figure 1C).[56−62] Introducing three identical substituents at the dissymmetric positions of its periphery, this bowl-shaped molecule becomes enantiomeric (if the substitutent is achiral) or diastereomeric (if the substitutent is chiral), and possesses three identical chiral microenvironments at the C_3-symmetric substitution positions.

Here, we explored substituting the C_3-symmetric positions of trioxatricornan with amino acid residues (Figure 2). This molecular structure provides a rich collection of intramolecular interactions including partial conjugation between the aromatic rings and the carbonyl group from the peptide bond, the potential intramolecular hydrogen bonds between the amide protons and the bridge oxygen, and possibly the steric effect between the side chains of the amino acid residues and the trioxatricornan moiety. Because of the close connectivity between these intramolecular interactions and the dissymmetric core, the molecular interactions have the potential to guide the overall molecule to adopt a well-defined minimum-energy structure.

Results and Discussion

Bromination of Trioxatricornan. The trioxatricornan core has been synthesized previously.[59,63] Lofthagen et al.[64] converted 4,8,12-trioxadibenzopyrene cation (Martin's salt)[60] to 12c-methyl-4,8,12-trioxatricornan, which was further functionalized to make a siderophore with C_{3v} symmetry. To make an amino acid-derivatized dissymmetric molecule with C_3 symmetry, we first coupled Martin's salt with different alkenyl Grignard reagents to afford bowl-shaped molecules (Scheme 1) followed by converting the alkenyl groups **1** to primary alcohols **2**. Compound **2a** was chosen for subsequent studies as it is furnished in higher yields when compared with **2b** and **2c**. Bromination of **2a** in chloroform resulted in 61% C_1 tribromosubstituted **3** and 34% C_3 tribromosubstituted **4** trioxatricornan.

TABLE 1. Temperature Effect on Bromination of Trioxatricornan

entry	R	solvent	temp, °C	C_1:C_3 isomer (yield, %)
1	$-CH_2CH_2OH$	$CHCl_3$	0	100:0 (60%, 0%)[b]
2[a]	$-CH_3$	HOAc	rt	100:10 (51%, 5%)
3	$-CH_2CH_2OH$	$CHCl_3$	rt	100:50 (61%, 34%)[b]
4	$-CH_2CH_2OH$	$CHCl_3$	60	100:0 (61%, 0%)[b]
5[a]	$-CH_3$	HOAc	80	100:33 (42%, 14%)

[a]Conditions reported previously.[59] [b]ratio for molecules **3** and **4**.

Statistical Control of Regioselectivity. The substitution reactions of trioxatricornan appear to be ortho-directed by the bridge oxygen, and lead to trisubstituted products that are predominantly C_1 symmetric rather than C_3 symmetric. This preference in regiochemistry is likely controlled by the statistics of the substitution as reaction progresses from monosubstitution to disubstitution and finally trisubstitution (see the Supporting Information). Without considering the small energy difference, the statistics prescribe a product ratio of 75:25 for C_1-symmetric and C_3-symmetric isomers. Our own efforts in bromination and past examples by Siegel and coworkers[57] which included other electrophilic aromatic reactions such as nitration with HNO_3, bromination with Br_2/HOAc, or silylation with *n*-BuLi/TMSCl of trioxatricornan, have resulted in ratios of the C_1-symmetric to C_3-symmetric isomers all around 75:25 (C_1:C_3).

(56) Laursen, B. W.; Krebs, F. C. *Angew. Chem., Int. Ed.* **2000**, *39*, 3432–3434.
(57) Lofthagen, M.; Chadha, R.; Siegel, J. S. *J. Am. Chem. Soc.* **1991**, *113*, 8785–8790.
(58) Lofthagen, M.; Siegel, J. S. *J. Org. Chem.* **1995**, *60*, 2885–2890.
(59) Lofthagen, M.; VernonClark, R.; Baldridge, K. K.; Siegel, J. S. *J. Org. Chem.* **1992**, *57*, 61–69.
(60) Martin, J. C.; Smith, R. G. *J. Am. Chem. Soc.* **1964**, *86*, 2252–2256.
(61) Mobian, P.; Nicolas, C.; Francotte, E.; Burgi, T.; Lacour, J. *J. Am. Chem. Soc.* **2008**, *130*, 6507–6514.
(62) Laursen, B. W.; Soerensen, T. J. *J. Org. Chem.* **2009**, *74*, 3183–3185.
(63) Faldt, A.; Krebs, F. C.; Thorup, N. *J. Chem. Soc., Perkin Trans. 2* **1997**, 2219–2227.
(64) Lofthagen, M.; Siegel, J. S.; Hackett, M. *Tetrahedron* **1995**, *51*, 6195–6208.

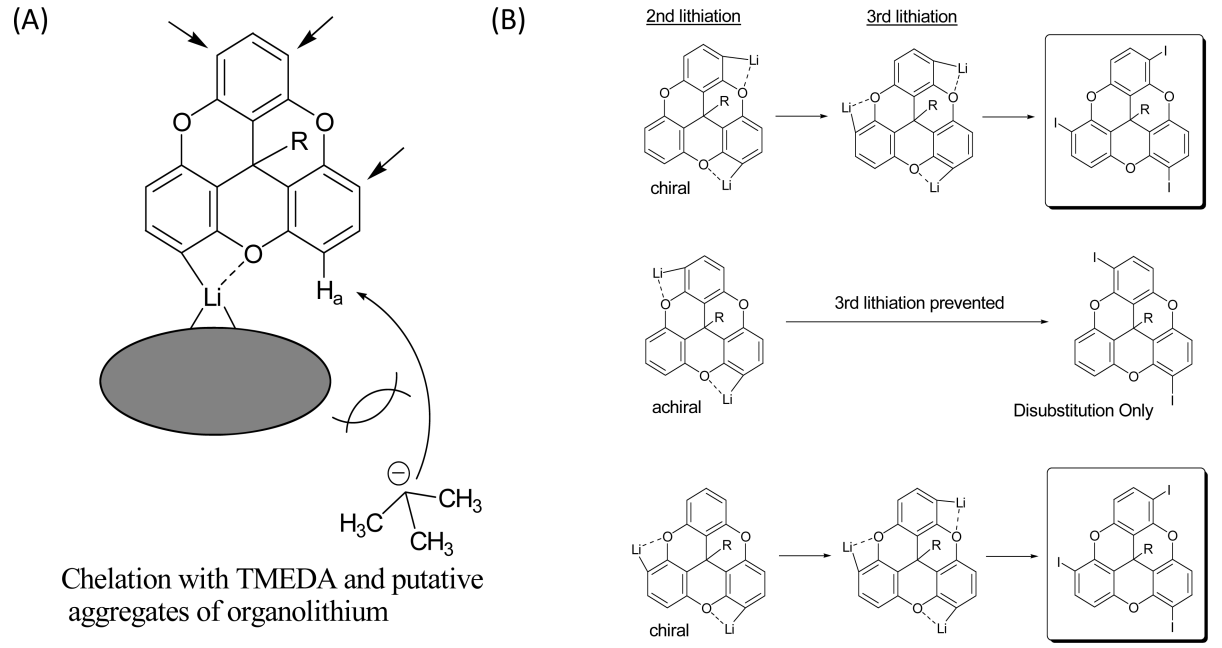

FIGURE 3. (A) The proposed model for preventing second lithiation on the neighboring proton (H_a) of trioxatricornan. The first ortho-directed lithiation provides either steric or electronic influence by the presumed chelation or organolithium-based aggregates, which prevents the second lithiation at the nearest neighboring site (H_a). The arrows indicate positions left possible for the second lithiation. (B) Substitution statistics controlled by stereoelectronic influence of TMEDA/*t*-BuLi.

SCHEME 2

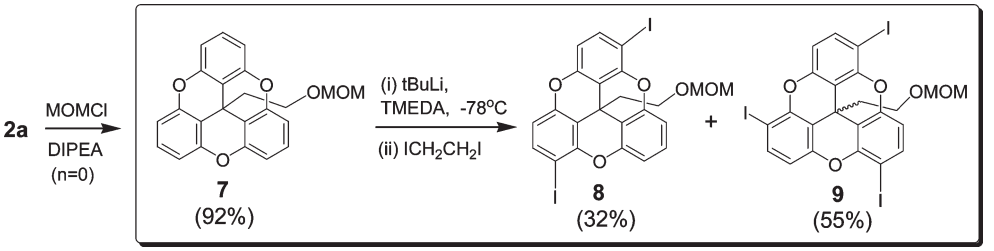

Table 1 shows the selected conditions and results for bromination of trioxatricornan. For all conditions, the C_1-symmetric isomer is the predominant product over the C_3-symmetric isomer. The exact ratio of the two depends on the experimental conditions. The most interesting observation for this reaction is its dependence on temperature. At both a low temperature (0 °C) and a high temperature (60−80 °C), the proportion of the C_3-symmetric isomer (0−14%) was significantly lower than the statistically predicted 25% (C_1:C_3 = 75:25), whereas at an ambient temperature the proportion of C_3-symmetric isomer can increase to 34%, which is higher than the statistically predicted 25% (see the Supporting Information). Calculations based on density functional theory (DFT)[65,66] suggest that the energy difference between the C_1-symmetric isomer and C_3-symmetric isomer is marginal, with the C_3 isomer being 0.2 kcal/mol lower than the C_1 isomer. However, based on the temperature effect on the substitution reaction in chloroform, we believe that the C_1-symmetric isomer is likely both the kinetic and thermodynamic product. At low temperature, we believe kinetic control dominates for this reaction, affording mostly the C_1-symmetric product; at intermediate temperature the C_3-symmetric product becomes more accessible while the reaction is still largely irreversible, and thus the increase in yield of C_3-symmetric product; at a sufficiently high temperature, the reaction becomes reversible and thermodynamic control dominates and affords predominately the C_1-symmetric product again.

Reversing the Regioselectivity. In this work, we are interested in how the repeated microenvironment at C_3-symmetric positions can couple with the stereogenic centers of the amino acid residues to induce folding in the molecule. To break the statistical influence and reverse the regioselectivity to obtain the desired C_3-symmetric isomer, we seek to introduce either steric and/or electronic influence on the trioxatricornan ring to prevent the disubstitution on the closest neighboring positions, which leads to an undesired C_1-symmetric isomer (Figure 3A). With use of MOM-protected trioxatricornan **7** (Scheme 2), ortho-lithiation[67−69] by *tert*-butyllithium and TMEDA followed by the addition of 1,2-diiodoethane validated this approach, which affords the

(65) Hohenberg, P.; Kohn, W. *Phys. Rev. B* **1964**, *136*, 864–871.
(66) Kohn, W.; Sham, L. *J. Phys. Rev. A* **1965**, *140*, 1133–1138.
(67) Gschwend, H. W.; Rodriguez, H. R. *Org. React.* **1979**, *26*, 1–360.
(68) Shimano, M.; Meyers, A. I. *J. Am. Chem. Soc.* **1994**, *116*, 10815–10816.
(69) Snieckus, V. *Chem. Rev.* **1990**, *90*, 879–933.

SCHEME 3

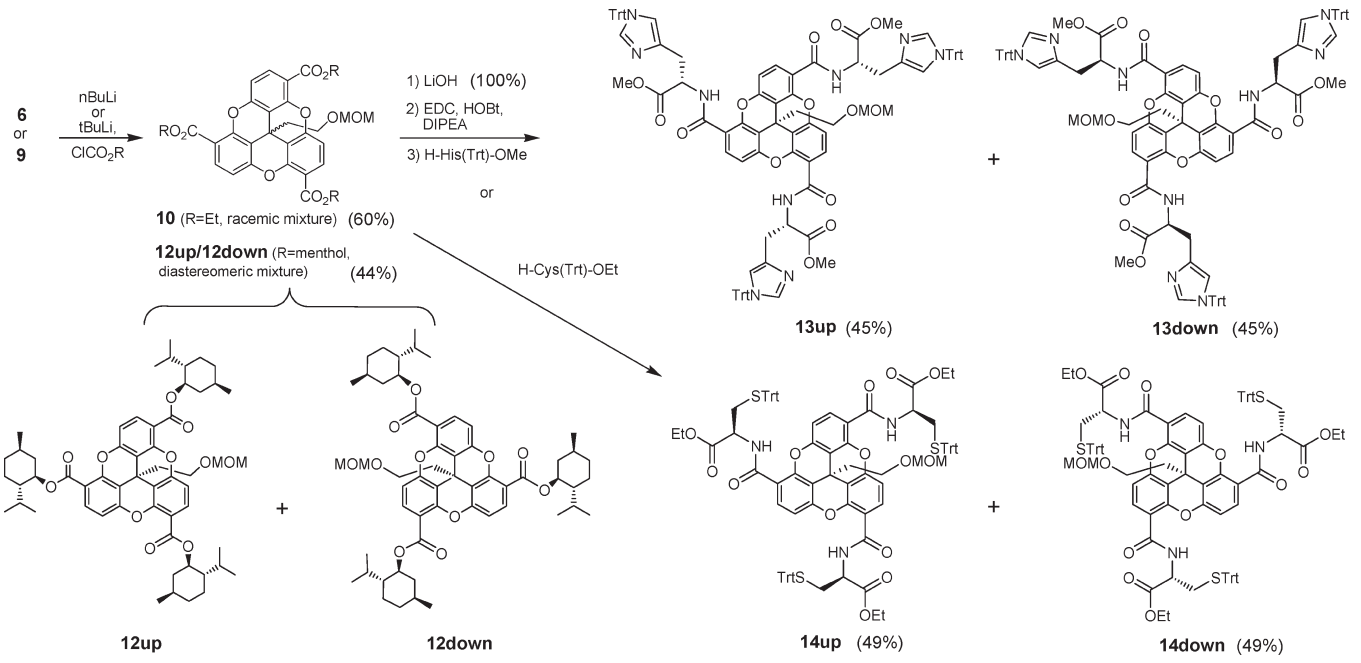

desired C_3-symmetric isomer of triiodo-substituted trioxatricornan, **9**, as the major product (isolated yield: 55%), and the diiodosubstituted isomers **8** containing a trace amount of chiral disubstitution product (total yield: 32%). No C_1-symmetric isomer was observed. Because the two closest protons on the two aromatic rings in trioxatricornan are about 4.7 Å apart, the approach of a second *tert*-butyllithium reagent to the aromatic hydrogen (H_a) closest to the first lithiation is prevented by either the steric hindrance of the bulky chelate (or the putative formation of organolithium aggregates)[70−73] or the lack of further chelation from the bridged oxygen for the second lithium cation.

Figure 3B describes a proposed reaction cascade of multiple lithiation that accounts for the product distribution. Two of the three possible positions for second lithiation afford the chiral dilithiated trioxatricornan, and the other one affords an achiral dilithiated trioxatricornan. Whereas the chiral dilithiated product proceeds with the third lithiation at the C_3-symmetric position, the achiral dilithiation product cannot proceed with a third lithiation because neither of the ortho positions on the third ring are accessible. This lithiation pattern leads to a ratio of 2:1 for the C_3-symmetric product and diiodo-substituted trioxatricornan, which is consistent with the observed yields. Direct carbonylation of trioxatricornan without any substituted halides also supported the proposed stereochemical control. Using normal butyllithium and *tert*-butyllithium followed by ethyl chloroformate resulted in overall low yield for the products, but with a ratio that showed reversal of the regiochemistry when *tert*-butyllithium is used. While using normal butyllithium afforded both C_1-symmetric (∼8%) and C_3-symmetric (∼5%) trisubstituted product, using the bulkier *tert*-butyllithium gave only C_3-symmetric product (∼8−10%) (see the Supporting Information). Using other electrophiles, including carbon dioxide, diethylcarbonate, or diphenylcarbonate, afforded only disubstituted products.

Synthesis and Resolvability of C_3-Dissymmetric Molecules. Using this controlled regiochemistry, we derivatized the trioxatricornan with esters and amino acids at C_3-symmetric positions, which resulted in a new class of C_3-symmetric diastereomers (Scheme 3). The trisubstituted trioxatricornan **6** (or **9**) was lithiated by *t*-BuLi and treated with ethylchloroformate or (−)-(1*R*)-menthylchloroformate to afford racemic **12up** and **12down**. Basic hydrolysis of **10** followed by amide bond formation with amino acid residues cysteine or histidine resulted in diastereomers of **13up** and **13down**, as well as **14up** and **14down**. The terms "**up**" or "**down**" denote the low or high polarity, respectively, as measured on the TLC, their correlation with the absolute configurations as shown are determined by using vibrational circular dichroism and density functional calculation, see below.

Resolution for Amino Acid Substituted Trioxatricornan Is Easier than That for (−)-Menthol Substituted of Trioxatricornan. L-Histidine and L-cysteine (1-(triphenylmethyl)-L-histidine methyl ester and triphenylmethyl-L-cysteine ethyl ester) were substituted on trioxatricornan at C_3-symmetric positions. For histidine and cysteine derivatized C_3-trioxatricornan, the top and bottom diastereomers **13up**/**13down** and **14up**/**14down** are easily resolvable by flash column chromatography. For trioxatricornan derivatized with menthyl ester **12up/12down**, the diastereomers are more difficult to separate than the amide diastereomers. The purification of **12up** and **12down** was accomplished by 14 repetitive runs on a preparative thin layer chromatography (PTLC) plate that employed 5% EtOAc in pentane.

(70) Beak, P.; Musick, T. J.; Liu, C.; Cooper, T.; Gallagher, D. J. *J. Org. Chem.* **1993**, *58*, 7330–7335.
(71) Gossage, R. A.; Jastrzebski, J. T. B. H.; van Koten, G. *Angew. Chem., Int. Ed.* **2005**, *44*, 1448–1454.
(72) Pratt, L. M. *Mini-Rev. Org. Chem.* **2004**, *1*, 209–217.
(73) Gruver, J. M.; Liou, L. R.; McNeil, A. J.; Ramirez, A.; Collum, D. B. *J. Org. Chem.* **2008**, *73*, 7743–7747.

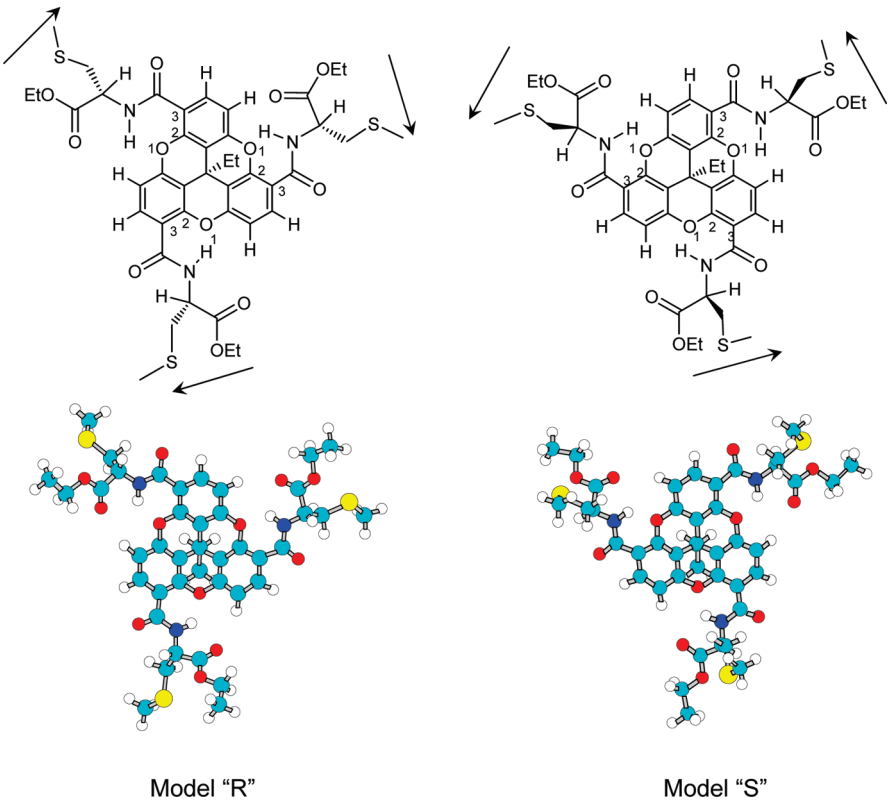

FIGURE 4. Assignment of handedness of the C_3 core (upper frame) and calculated optimized geometries (lower frames, Gaussian 03: DFT B3LYP/6-31G(d) level) for diastereomer models "R" and "S" for comparison with samples **14up** and **14down**. Cores are viewed here concave-up, with the ethyl group below the core. The arrows and the numbering show the priority for assigning "R" and "S" absolute configurations.

SCHEME 4

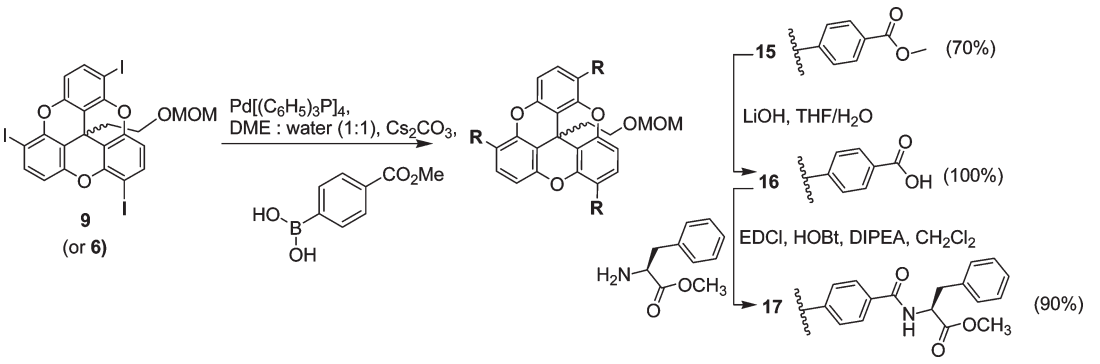

Increasing the Distance between the Stereogenic Center and the Trioxatricornan Core Reduces Resolvability. Substituting a rigid phenyl linker between the amino acid and the trioxatricornan moiety afforded diastereomers **17** (Scheme 4). Multiple elutions with various solvent systems on the same TLC plates did not afford any observable separation for these diastereomers. Furthermore, whereas the chemical shifts in proton NMR are different between each of the three pairs of diastereomers described above, the chemical shift of aromatic protons in **17** showed a clean set of four doublets: two doublets arise from the two chemically equivalent sets of protons on the aromatic rings of trioxatricornan and the remaining two doublets arise from the identical phenyl linkers. These results suggest that the stereogenic centers of the amino acids are not coupled with the dissymmetry of the central fused aromatic rings.

Vibrational Circular Dichroism (VCD) of the Diastreomers of 13 and 14. To determine the absolute configurations of **14up**, **14down**, **13up**, and **13down**, vibrational circular dichroism (VCD)[74] spectra was measured for samples in $CDCl_3$ solution and compared to the calculations (DFT level, B3LYP functional, 6-31G(d) basis set) for the model structures for diastereomers of **14** shown in Figure 4. For the purpose of assigning the absolute configuration, we use the following guidelines to describe the handedness of C_3-dissymmetric molecules. Our analysis involves (1) viewing along the C_3 axis through the concave face and (2) deducing the priority of atoms on the periphery of the ring from high to low using the

(74) Freedman, T. B.; Cao, X.; Dukor, R. K.; Nafie, L. A. *Chirality* **2003**, *15*, 743–758.

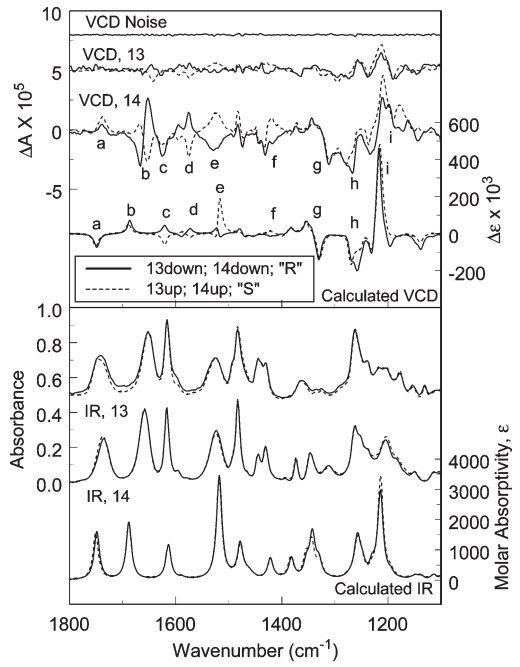

FIGURE 5. IR (lower frame) and VCD (upper frame) spectra observed for **13up/13down** and **14up/14down** (left axes, 3−5 mg sample/150 μL $CDCl_3$) compared to calculation for diastereomer models "R" and "S" (right axes, DFT B3LYP functional/6-31G(d) basis set). Solid lines are spectra for **13down**, **14down**, and "R"; dotted lines are spectra for **13up**, **14up**, and "S". Uppermost trace is VCD noise for **14up**.

guidelines established by Cahn-Ingold and Prelog.[75] If the direction of precedence along the periphery is clockwise, then the handedness is designated as "R"; if the direction is anticlockwise, then the handedness is designated as "S".

The experimental IR and VCD spectra of **14up**, **14down**, **13up**, and **13down** in $CDCl_3$ solution are compared to the calculation in Figure 5 for the 1800−1100 cm^{-1} region. The IR spectra of each pair of samples overlay closely, indicative of similar high purity for each pair, and the VCD spectra show bands that are representative of diastereomers in the given spectral range, indicative of similar optical purity for each pair. The VCD spectra were obtained with a very good signal-to-noise ratio ($\Delta A \approx 10^{-6}$).

The calculated IR spectra agree well in pattern with the observed, providing evidence that the normal vibrational modes are well-produced at this DFT level of calculation. Some of the differences between observed and calculated IR spectra arise from modes of the peripheral alkyl groups truncated to generate the model. The experimental VCD spectra of **13** show regions of opposite sign for the diastereomers (regions "b", "c", "d", "e", and "f" in Figure 5) that reflect the opposite propeller configurations of the diastereomers, and regions with similar VCD pattern (regions "a", "g", "h", and "i" in Figure 5) that have large contributions from vibrations of the L-amino acid substituents. The coupled vibrations under C_3 symmetry give rise to A and E symmetry species components that produce a VCD couplet of opposite sense for the two propeller configurations, as demonstrated by couplet "b" for the peptide C=O stretches.

(75) Cahn, R. S.; Ingold, C.; Prelog, V. *Angew. Chem., Int. Ed. Engl.* **1966**, *5*, 385–415.

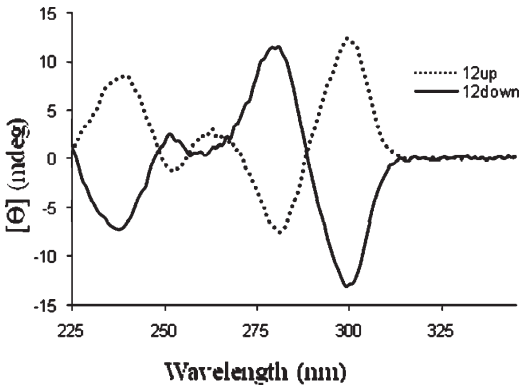

FIGURE 6. ECD spectra for "S" and "R" trioxatricornan cores derivatized with (−)-menthol (**12up** and **12down**) collected at room temperature in a 1.0 cm path length quartz cell. ECD signals were measured at 1 nm intervals with averaging times of 5s/nm. The spectral bandwidth was 1.5 nm. Sample concentrations were 0.074 (**12up**) and 0.068 μM (**12down**) in THF.

In other regions with large contributions from aromatic ring deformations, such as "c", "d", "e", and "f", the A and E components are not resolved, and the VCD reflects the net intensity bias of the couplet, yielding near mirror-image VCD signals for the diastereomers. For regions "g", "h", and "i", the large contribution of methine deformations at the L-amino acid chiral centers is the dominant determinant of the VCD signal, and mode a is primarily the ester C=O stretch; for these normal modes, the propeller sense changes only the magnitude, but not the sign of the VCD. The experimental VCD spectra for **13** show VCD patterns similar to those of **14**, but considerably weaker in magnitude.

The calculated VCD spectra are for model diastereomers for **14**, each in a single conformation. The large size of the molecules under investigation precludes VCD calculation of the entire structure and identification of the large number of solution conformers possible for the model structures. The conformations of models "R" and "S" include stabilization by intramolecular hydrogen bonding between the peptide NH and diaryl ether oxygen of the C_3 core (a 180° rotation of the peptide produces a conformation much higher in energy) and weak intramolecular hydrogen bonding between NH and ester C=O, one of the many possible conformations for the amino acid centers. For both **14up**/**14down** and **13up**/**13down**, the NH stretch was measured at 3420 cm^{-1}, consistent with a moderate to weak nonlinear hydrogen bond. Despite the limitations of the models, the calculated VCD spectra reproduce many of the observed VCD intensity pattern differences for the diastereomers (regions "c", "d", "e", "f", "h"), and the overall VCD patterns and smaller differences in the region with large amino acid methine deformation contributions (below 1400 cm^{-1}). For region b, the calculated A and E components for the peptide C=O stretch are not resolved as well as in the experimental spectrum; however, the sense of the couplet, (−,+) for "R", (+,−) for "S", is reproduced in the calculated intensities for the A and E components, and this sense confirms the orientation of the peptide and consequent NH--O intramolecular hydrogen bonding for the experimental samples. For region "a", the VCD calculation is opposite in sign to that observed. The VCD of this ester C=O stretch is sensitive to orientation of the ester group. The observed positive VCD for region "a"

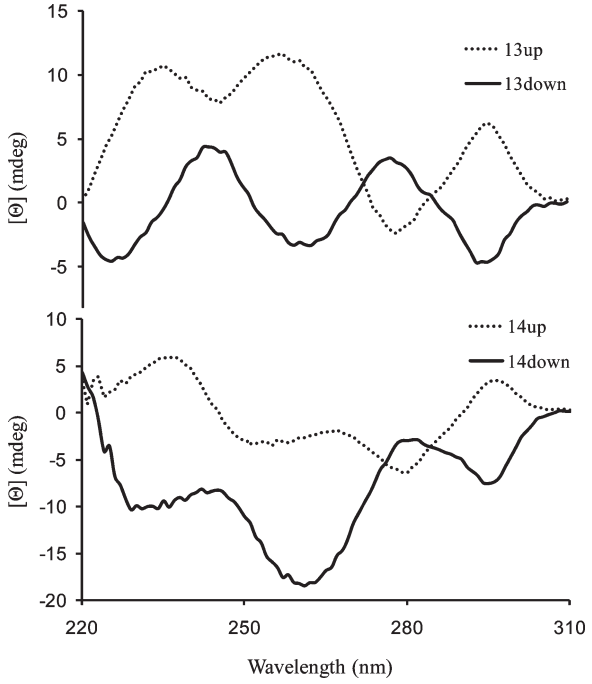

FIGURE 7. ECD spectra of for "S" and "R" trioxatricornan core derivatized with L-histidine (**13up** and **13down**) or with L-cysteine (**14up** and **14down**) collected at room temperature in a 1.0 cm path length quartz cell. ECD signals were measured at 1 nm intervals with averaging times of 5s/nm. The spectral bandwidth was 1.5 nm. Sample concentrations were 138 μM for **13up**, 123 μM for **13down**, 10 μM for **14up**, and 10 μM for **14down** in THF.

suggests a prevalence of other orientations for the amino acid ester substituents, such as those deduced for a conformationally averaged structure by NMR (structure derived by molecular dynamics). The weaker VCD signal (relative to the IR) for diastereomers **13** compared to **14** suggests lower optical purity and/or much greater conformational flexibility for **13**. However, the observed VCD pattern differences between **13up** and **13down** also correspond to the calculated VCD differences between models "R" and "S".

The comparison between observed VCD spectral patterns for **13** and **14** and the calculated VCD spectra for models "R" and "S" provides assignment of **13up** and **14up** to "S" and assignment of **13down** and **14down** to "R" for the absolute configurations of the core of the C_3-symmetric trioxatricornan.

Electronic Circular Dichroism (ECD) of the Diastreomers of 12, 13, and 14. The diastereomers of **12up** and **12down** exhibited electronic circular dichroism with remarkable mirror-image characteristics. For **12up**, three bands in the ECD spectra centered at 238, 262, and 300 nm show positive Cotton effects; for **12down**, three bands were also seen centered at 238, 261, and 300 nm with the same intensity magnitude, but exhibited negative Cotton effects. Furthermore, diastereomer **12up** exhibited two bands centered at 252 and 281 nm with negative Cotton effects, and diatereomer **12down** also exhibited two bands centered at 252 and 279 nm but with positive Cotton effects (Figure 6). This remarkable mirror-image characteristic for the ECD for **12up** and **12down** indicates that even though **12up** and **12down** are diastereomers, the electronic transitions of the saturated menthol group are too high in energy to contribute to the

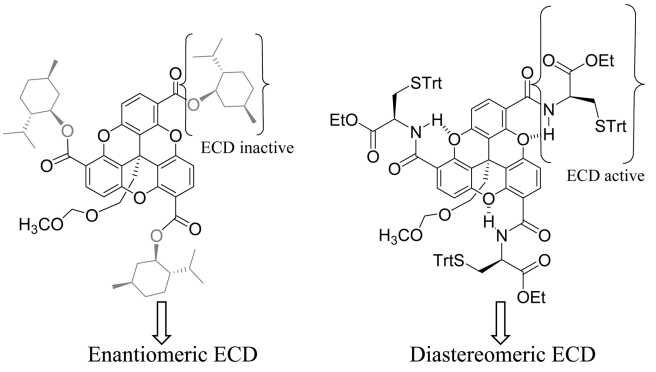

FIGURE 8. Effect of chiral substituents on the ECD signal; the trioxatricornan core and the amino acid residues are ECD active but the menthol groups are not.

electronic transitions in this region, but the remainder of the trioxatricornan group with three carbonyl groups are enantiomeric and are active for ECD (Figure 8).

The ECD of **13up/13down** and **14up/14down** show a common pattern, but do not exhibit mirror-image characteristics (Figure 7). The ECD spectra of **13up** and **14up** show positive Cotton effects with bands centered at 238, 260, 296 nm and 235, 266, 296 nm, respectively, and negative Cotton effects with bands at 248, 280 nm and 253, 279 nm, respectively. Similarly, **13down** and **14down** show positive Cotton effects at bands centered at 247, 279 nm and 243, 279 nm, respectively, and negative Cotton effects with bands centered at 230, 262, 295 nm and 230, 260, 295 nm, respectively. Overall, the electronic CD transitions occur at similar wavelengths, but with different intensities, which is consistent with the diastereomeric nature between **13up**/**13down** and **14up**/**14down** where the peptide conjugation with the trioxatricornan and proximity to the chiral amino acid directly contribute in this spectral region. We note that the bands for the high wavelengths from 279 to 295 nm did exhibit similar intensity with opposite Cotton effect for each pair of diastereomers.

Compared with absolute configuration determined by the VCD, these results suggest that there is a common relation between the absolute configuration and the electronic circular dichroism for these molecules. For example, both **13up** and **14up** have "S" configuration and a positive ECD band at 296 nm, and both **13down** and **14down** have "R" configuration and a negative ECD band at 295 nm.

Determination of Absolute Configuration of the Diastereomers 12up and 12down by ECD Inferences. Examining the bands in the ECD suggests that the bands in **13up** [(+) Cotton at 238, 260, and 296 nm and (−) Cotton at 248 and 280 nm] and **14up** [(+) Cotton at 235, 266, and 296 nm and (−) Cotton at 253 and 279 nm] are very similar to bands observed in **12up** [(+) Cotton at 238, 262, and 300 nm and (−) Cotton at 252 and 281 nm]. Likewise, the bands in **13down** [(+) Cotton at 247 and 279 nm and (−) Cotton at 230, 262, and 295 nm] and **14down** [(+) Cotton at 243 and 279 nm and (−) Cotton at 230, 260, and 295 nm] are very similar to bands observed in **12down** [(+) Cotton at 252 and 279 nm and (−) Cotton at 238, 261, and 300 nm]. Because the observed correlation between the absolute configuration and the pattern of ECD for **13up/13down** and **14up/14down**, and because similar patterns in ECD are seen for **12up** and **12down** (especially at long wavelength, ~296−300 nm), we

TABLE 2. Correlation between Observed Polarity, Cotton Effects from ECD, and Absolute Configuration of Diastereomers of 12, 13, and 14

	14up	14down	13up	13down	12up	12down
[a]polarity (R_f)	[b]0.48	[b]0.32	[c]0.27	[c]0.19	[d]0.43	[d]0.38
Cotton effect (wavelengths)	positive (296 nm)	negative (295 nm)	positive (296 nm)	negative (295 nm)	positive (300 nm)	negative (300 nm)
absolute configuration	[e]S	[e]R	[e]S	[e]R	[f]S	[f]R

[a]R_f values from thin layer chromatography (TLC). [b]Eluents for TLC: 50% EtOAc in Hexanes. [c]Eluents: 4% MeOH in CH_2Cl_2. [d]Eluents: 5% EtOAc in pentane. [e]Determined by vibrational circular dichroism and DFT calculation. [f]Determined by indirect inference from electronic circular dichroism.

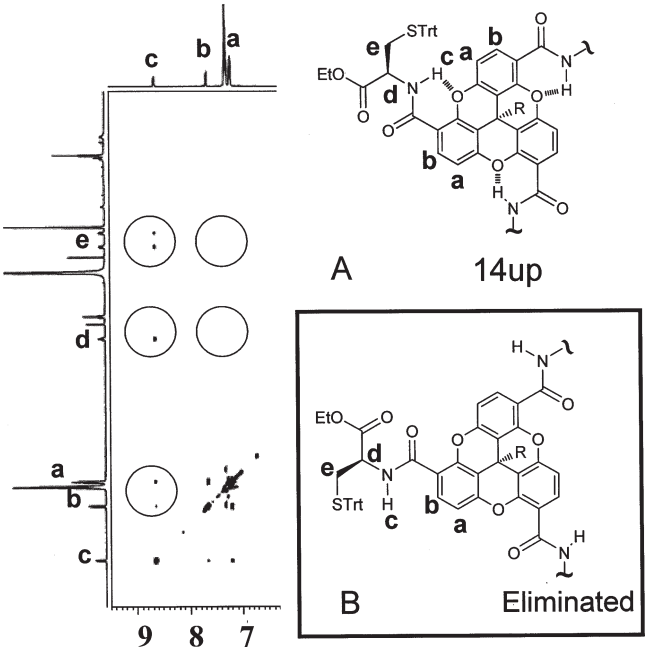

FIGURE 9. NOESY spectrum of **14up** in DMSO-d_6 shows the relayed NOE from protons a to b to c to d to e, which supports conformation "A". The NOESY spectrum for **14down** exhibited identical NOE correlations (see the Supporting Information).

infer that the menthyl ester diastereomer **12up** has the "S" absolute configuration for the trioxatricornan core, the same as that for **13up** and **14up**. The diastereomer **12down** has the "R" absolute configuration, the same as that for **13down** and **14down**. Together with the TLC results, this inference also results in the "S" diastereomers being less polar than the "R" for the conformations on the TLC plate.

We note that the polarity, based on TLC, reveals that, for the diastereomers studied in this work, the "R" configuration in the core is consistently more polar than the "S" configuration. Table 2 summarizes the observed polarity, Cotton effect of ECD at long wavelength, and the absolute configurations of the diastereomers.

NMR Analysis of the Structures of the Diastereomers. Chemical shifts of protons in each pair of the resolved diastereomers were different. For example, protons (b) exhibited a chemical shift at 8.13 ppm for **14up**, but 7.93 ppm for **14down** in $CDCl_3$. Even for diastereomers of menthol derivatized trioxatricornan that were difficult to resolve by column chromotography, the aromatic protons exhibited a difference in chemical shifts of 0.03 ppm in $CDCl_3$ (see the Supporting Information). These results suggest that the protons are in different microenvironments on each diastereomer.

The Nuclear Overhauser Enhancement Spectroscopy (NOESY) experiments for amino acid derivatized diastereomers **14up** and **14down** were conducted in both DMSO-d_6 and $CDCl_3$. The diastereomers exhibited identical patterns of NOE correlations in both solvents. Figure 9 shows the NOESY spectrum for **14up** in DMSO-d_6 with a mixing time of 1.2 s; the NOESY spectrum for **14down** is included in the Supporting Information. No long-range NOEs between aromatic protons (a and b) and amino acid residue protons (d and e) were observed for both of the diastereomers (see the Supporting Information).

Without ring constraint, a secondary amide bond, in general, does not exist in the "E" configuration.[76−78] The "Z" configuration can be favored by roughly 2 kcal/mol relative to the "E" configuration.[77,79] Because of the partial conjugation of the carbonyl group with the aromatic ring, the "Z" amide bonds in diastereomers **14up** and **14down** can adopt a conformation of either "A" or "B" form (Figure 9). Both of the conformations "A" and "B" prevent the protons on the amino acid residues (d and e) from being in close proximity to aromatic protons (a and b) for an NOE correlation. These NOEs were not observed. We note that, if the diastereomers adopt "E" amide bonds for either rotamers concerning the aromatic−carbonyl C−C bond, the amino acid protons and the aromatic protons on the trioxatricornan ring will be in close enough promixity for an NOE correlation.

For conformation "A" with "Z" amide configuration, the amide proton (c) is closer to the aromatic proton (a) than to proton (b); whereas for conformation "B", the amide proton (c) is closer to aromatic proton (b) than to proton (a). Thus, the NOE correlation characterizing the distances between these two sets of protons (amide proton c to aromatic protons a or b) should distinguish between conformations "A" and "B". Examining the NOESY shown in Figure 9 indicated that the NOE signal between amide proton (c) and aromatic proton (a) is about 1.5 time stronger than that between proton (c) and aromatic proton (b). This bias in NOE intensity was observed in the NOESY spectra for both **14up** and **14down** in DMSO-d_6 and in $CDCl_3$ (see the Supporting Information). Thus, we conclude that conformation "A" rather than "B" is preferred for both of the diastereomers. Because of the close promixity, conformation "A" is also consistent with the existence of intramolecular hydrogen bonding between the N−H proton and the bridged oxygen on the trioxatricornan core.

To assess the local conformation and the spatial location of substituted amino acid residues relative to the chiral aromatic core of **14up** and **14down**, the relay NOEs between protons (a/b to c), (c to d/e), and the torsional angles that define the bond H−N−C*−H were examined. The NOEs between protons (a/b to c) and (c to d/e) are similar in their

(76) Gardner, R. R.; McKay, S. L.; Gellman, S. H. *Org. Lett.* **2000**, *2*, 2335–2338.
(77) Stewart, W. E.; Siddall, T. H. III *Chem. Rev.* **1970**, *70*, 517–51.
(78) Weiss, M. S.; Jabs, A.; Hilgenfeld, R. *Nat. Struct. Biol.* **1998**, *5*, 676.
(79) Radzicka, A.; Pedersen, L.; Wolfenden, R. *Biochemistry* **1988**, *27*, 4538–4541.

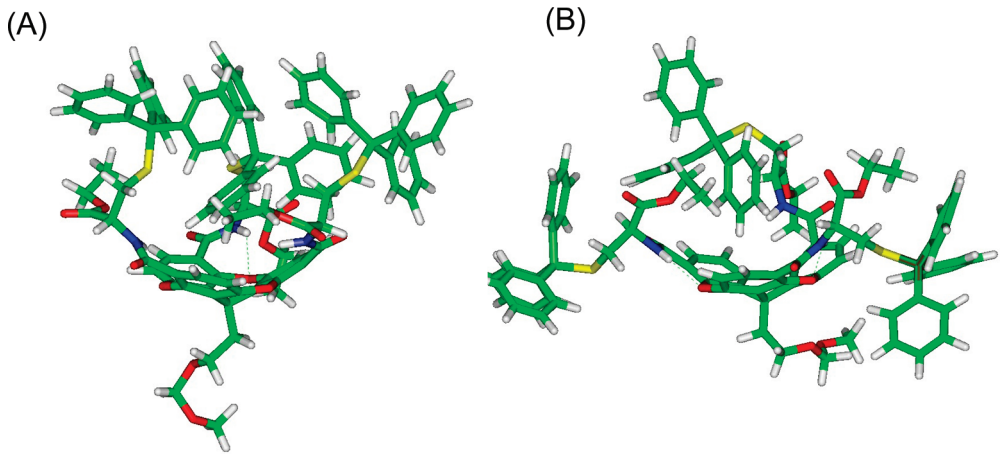

FIGURE 10. NMR derived structures for diastereomers in vacuum: (A) **14up** is folded toward the interior of the cavity and (B) **14down** has an open folded structure.

intensities (see the Supporting Information). The averaged coupling constants ($^3J_{H-N-C-H}$) for the N−C* bonds in the amino acid residues of the two diastereomers were close; 7.43 Hz for **14up** and 7.28 Hz for **14down**, implying a similar range of torsional angles for both of the diastereomers. Together, these results suggest that the local conformations of the amino acid residues in both diastereomers are comparable.

Because the substituted amino acids are of a pure L-configuration, substitutions at C_3-symmetric (chiral) positions are diastereotopic. Furthermore, because the local conformations of the amino acids are similar, the absolute "S" or "R" configuration of the core structure will govern how the amino acid residues are oriented relative to the trioxatricornan core. Specifically, the "S" enantiomer with conformation "A" will orient the cysteine residue toward the concave cavity of the trioxatricornan core, whereas the "R" enantiomer will orient the cysteine outside the cavity of the trioxatricornan core. We note that, although these NOE signals, together with difference in polarity of the molecules, suggest different folded structures for the two diastereomers, the amino acid residues may afford more dynamic, albeit restricted, local conformations due to the thermal fluctuation and freedom in the rotation of N−C* bonds.

We applied molecular dynamics (MD) using experimental parameters generated by NOESY experiments for the two diastereomers, **14up** and **14 down**. These calculations were performed in a vacuum (using DISCOVER module in Insight Program)[80] and with solvents including $CHCl_3$ and DMSO (using AMBER 10).[81] The two diastereomers show different global structures. In the vacuum, the energy-minimized structures for both diastereomers have "Z" rotamers for the amide bonds, and identical core structures. In diastereomer **14up**, the side chains of the amino acids fold toward the center of the chiral core; in **14down**, the side chains of the amino acids spread outward from the ring periphery (Figure 10). We note that the amino acid residues exhibit a more dynamic range although their orientations remain differently relative to the trioxatricornan core. MD simulations for both diastereomers in solvents are in agreement with the minimized structures obtained in the vacuum (see the Supporting Information). Furthermore, for all the calculated structures, the amide proton (c) and the bridged oxygen atoms are in close proximity to each other, within a distance consistent with the existence of intramolecular hydrogen bonds. The calculated N−H---O bond distances for **14up** are 2.0, 2.27, and 1.98 Å, and for **14down** they are 2.27, 2.54, and 2.07 Å. The existence of intramolecular hydrogen bonds is further supported by the observation that the downfield signals arising from amide N−H protons were not perturbed significantly ($\Delta\delta$(NH) < 0.25 ppm) when the solvent was changed from $CDCl_3$ to DMSO-d_6.[82,83]

Conclusions

We have synthesized a new class of chiral bowl-shaped C_3-symmetric trioxatricornan molecules. Without deliberate control, the regioselectivity for the tribromination of trioxatricornan is dominated by the statistical outcomes to afford predominately C_1-symmetric tribromo trioxatricornan. We reversed this statistically dominating regioselectivity by using bulky lithiation reagents to afford predominately C_3-symmetric triiodosubstituted trioxatricornan in good yields without the C_1-symmetric triiodo product. Derivatizing the C_3-symmetric halogenated trioxatricornans with L-amino acids or (−)-menthol afforded diastereomers that can be resolved by column chromatography. The absolute configurations for the resolved diastereomers have been determined by a combination VCD and DFT calculation, or ECD inference. Consistent among the three pairs of the diastereomers, the "R" configuration for the trioxatricornan core is more polar than the "S" configuration.

The similar NOE signals suggest that the two diastereomers adopt highly similar enantiomeric core structures, in which the amide hydrogen is close to the aryl hydrogen on the trioxatricornan that is adjacent to the bridged oxygen.

(80) Accelrys Software Inc., San Diego, CA.

(81) Case, D. A.; Darden, T. A.; Cheatham, T. E.; Simmerling, C. L.; Wang, J.; Duke, R. E.; Luo, R.; Crowley, M.; Walker, R. C.; Zhang, W.; Merz, K. M.; Wang, B.; Hayik, S.; Roitberg, A.; Seabra, G.; Kolossváry, I.; Wong, K. F.; Paesani, F.; Vanicek, J.; Wu, X.; Brozell, S. R.; Steinbrecher, T.; Gohlke, H.; Yang, L.; Tan, C.; Mongan, J.; Hornak, V.; Cui, G.; Mathews, D. H.; Seetin, M. G.; Sagui, C.; Babin, V.; Kollman, P. A.; *AMBER*, 10th ed.; University of California: San Francisco, CA, 2008.

(82) Le Grel, P.; Salauen, A.; Mocquet, C.; Le Grel, B.; Roisnel, T.; Potel, M. *J. Org. Chem.* **2008**, *73*, 1306–1310.

(83) Kopple, K. D.; Ohnishi, M.; Go, A. *Biochemistry* **1969**, *8*, 4087–4095.

Because of the NOE relay between the amide hydrogen and the protons in the amino acid residue, this core structure further defines the conformation ensemble of the substituted amino acids and the global folding of the structure. As a result, this work identified a folding moiety that consists of stereogenic centers connected by semirigid bonds to nonplanar aromatics. We believe that these chiral bowls have the potential for use in building novel supramolecular assembly and mimicking functional biological molecules.

Experimental Section

1,5,9-Triiodo-12c-(2-(methoxymethoxy)ethyl)-4,8,12-trioxatricornan (9). To a suspension of **7** (0.110 g, 0.294 mmol) in 5 mL of ether at −78 °C was added TMEDA (0.70 mL, 4.70 mmol). Then, to the resulting mixture, *t*-BuLi (1.7 M, 2.76 mL) was added dropwise to give a pale yellow turbid solution that was slowly warmed to 0 °C and stirred for 12 h. At this juncture, 1,2-diiodoethane (2.55 g, 9.05 mmol) in 5 mL of ether was introduced via cannula into the reaction flask and the mixture was stirred for another 12 h. The reaction mixture was quenched with 20 mL of water and extracted with EtOAc (2×100 mL). The organic layers were collected, washed with brine (25 mL), dried over Na_2SO_4, and concentrated in vacuo. Flash column chromatography (SiO_2, 10% EtOAc in hexanes) yielded 0.119 g of compound **9** (55%) as a white solid. R_f 0.4 (15% EtOAc in hexanes); ^{1}H NMR (300 MHz, $CDCl_3$) δ 7.73 (d, J = 8.7 Hz, 3H), 6.93 (d, J = 8.7 Hz, 3H), 4.39 (s, 2H), 3.40 (t, J = 6.6 Hz, 2H), 3.24 (s, 3H), 2.11 (t, J = 6.6 Hz, 2H); ^{13}C NMR (300 MHz, $CDCl_3$) δ 153.2, 151.8, 138.2, 114.4, 114.0, 97.1, 63.7, 55.8, 44.5, 30.1, 29.1; HRMS calcd for $C_{23}H_{15}I_3O_5$ [M]Na^+ 774.7945, found 774.7960.

1,5,9-Tri[(−)-(1*R*)-menthyl ester]-12c-(2-(methoxymethoxy)-ethyl)-4,8,12-trioxatricornan Diastereomers (12up and 12down). To a solution of **6** (0.100 g, 0.109 mmol) in dry THF (1.5 mL) was added *n*-butyllithium (1.6 M, 0.34 mL, 0.544 mmol) dropwise under argon atmosphere at −78 °C with stirring. After 3 h (−)-(1*R*)-menthylchloroformate (0.62 mL, 2.89 mmol) was added quickly at 0 °C. The solution was slowly warmed to rt and stirred for a further 8 h. The reaction mixture was quenched with saturated NH_4Cl solution (20 mL) and extracted with EtOAc (2 × 50 mL). The organic layers were collected, washed with brine (25 mL), dried over Na_2SO_4, and concentrated in vacuo. Flash column chromatography (SiO_2, 5−10% EtOAc in hexanes) yielded 0.066 g of a mixture of two diastereomers (44%) as a white greasy solid. The two diastereomers give a single spot (R_f 0.43; 10% EtOAc in hexanes). Further resolution was accomplished by 5 TLC runs (4% EtOAc in hexanes) yielding **12up** (R_f 0.43) and **12down** (R_f 0.38). Subsequent purification and isolation was accomplished by Preparative Thin Layer Chromatography (PTLC) that employed 5% EtOAc in pentane and after 14 repeated runs afforded **12up** and **12down** as a white powder.

12up: ^{1}H NMR (300 MHz, $CDCl_3$) δ 7.95 (d, J = 8.7 Hz, 3H), 7.03 (d, J = 8.7 Hz, 3H), 4.99 (m, 3H), 4.36 (s, 2H), 3.36 (t, J = 6.8 Hz, 2H), 3.19 (s, 3H), 2.17−1.09 (m, 27H), 1.0−0.80 (m, 27H); ^{13}C NMR (300 MHz, $CDCl_3$) δ 164.6, 155.3, 152.1, 132.4, 115.9, 113.0, 112.4, 97.2, 77.6, 63.9, 55.7, 47.8, 44.6, 41.5, 34.7, 31.9, 27.6, 26.5, 23.7, 22.8, 21.4, 16.6; HRMS calcd for $C_{56}H_{72}O_{11}$ [M]Na^+ 943.4967, found 943.4952.

12down: ^{1}H NMR (300 MHz, $CDCl_3$) δ 7.92 (d, J = 8.7 Hz, 3H), 7.05 (d, J = 8.7 Hz, 3H), 4.99 (m, 3H), 4.35 (s, 2H), 3.38 (t, J = 6.8 Hz, 2H), 3.18 (s, 3H), 2.14−1.07 (m, 27H), 0.98−0.80 (m, 27H); ^{13}C NMR (300 MHz, $CDCl_3$) δ 164.5, 155.2, 152.1, 132.2, 116.0, 113.0, 112.4, 97.1, 77.6, 63.8, 55.7, 47.8, 44.5, 41.4, 34.7, 31.9, 27.5, 26.7, 23.8, 22.5, 21.3, 16.7; HRMS calcd for $C_{56}H_{72}O_{11}$ [M]Na^+ 943.4967, found 943.4946.

1,5,9-Tri(*S*-trt-L-cysteine ethyl ester)-12c-(2-(methoxymethoxy)ethyl)-4,8,12-trioxatricornan Diastereomers (14up and 14down). To a solution of the crude acid (0.021 g, 0.041 mmol) and *S*-trt-L-cysteine ethyl ester (0.049 g, 0.125 mmol) in dichloromethane (2.0 mL) at 0 °C was added EDC·HCl (1-ethyl-3-(3-dimethylaminopropyl)carbodiimide) (0.077 g, 0.401 mmol) followed by HOBt (*N*-hydroxybenzotriazole monohydrate) (0.065 g, 0.481 mmol). The reaction mixture was stirred overnight and then quenched with water (5 mL) and extracted with EtOAc (2 × 50 mL). The organic layers were collected, washed with brine (25 mL), dried over Na_2SO_4, and concentrated in vacuo. Flash column chromatography (SiO_2, 40−60% EtOAc in hexanes) yielded 0.032 g of **14up** (49%) and 0.032 g of **14down** (49%) as off-white solids; R_f 0.48 (50% EtOAc in hexanes) for **14up** and R_f 0.32 (50% EtOAc in hexanes) for **14down**. Subsequent purification and isolation was accomplished by preparative thin-layer chromatography (PTLC) that employed 20% pentane in ether and afforded **14up** and **14down** diastereomers as a white powder.

14up: ^{1}H NMR (300 MHz, $CDCl_3$) δ 8.58 (d, J = 7.1 Hz, 3H), 8.13 (d, J = 8.8 Hz, 3H), 7.44−7.20 (m, 48H), 4.96 (m, J = 7.1 Hz, 3H), 4.30 (s, 2H), 4.34−4.24 (m, 6H), 3.48 (t, J = 6.5 Hz, 2H), 3.08 (s, 3H), 2.91−2.80 (m, 6H), 2.25 (t, J = 6.5 Hz, 2H), 1.31 (t, J = 7.1 Hz, 9H); ^{13}C NMR (300 MHz, $CDCl_3$) δ 170.9, 163.0, 154.0, 150.6, 144.7, 132.8, 129.9, 128.4, 127.3, 117.5, 113.3, 112.5, 97.2, 67.1, 63.9, 62.4, 55.8, 52.3, 34.7, 28.1, 14.6; HRMS calcd for $C_{98}H_{87}N_3O_{14}S_3$ [M]Na^+ 1648.5242, found 1648.5304.

14down: ^{1}H NMR (300 MHz, $CDCl_3$) δ 8.45 (d, J = 7.4 Hz, 3H), 7.93 (d, J = 8.8 Hz, 3H), 7.37−7.13 (m, 48H), 5.00 (m, J = 7.4 Hz, 3H), 4.33 (m, J = 7.1 Hz, 8H), 3.38 (m, J = 6.3 Hz, 2H), 3.17 (s, 3H), 2.94−2.74 (m, J = 4.7, 12.1 Hz, 6H), 2.16 (t, J = 6.3 Hz, 2H), 1.35 (t, J = 7.1 Hz, 9H); ^{13}C NMR (300 MHz, $CDCl_3$) δ 170.9, 162.9, 153.9, 150.5, 144.7, 132.7, 129.8, 128.5, 127.4, 117.5, 113.3, 112.5, 97.1, 67.2, 63.8, 62.5, 55.8, 52.0, 34.7, 28.0, 14.7; HRMS calcd for $C_{98}H_{87}N_3O_{14}S_3$ [M]Na^+ 1648.5242, found 1648.5206.

Acknowledgment. We thank the Chemistry Department at SU, the Syracuse Center for Excellence CARTI award supported by the U.S. Environmental Protection Agency [Grant X-83232501-0], and the NSF-CMMI (Grant No. 0727491) for partial financial support. We thank Professor Michael B. Sponsler (SU) for fruitful discussions, Professor S. Loh (SUNY Upstate Medical University) for the use of the CD instrument, and Professor Laurence A. Nafie (SU) for use of the VCD spectrometer.

Supporting Information Available: Experimental procedures and spectroscopic and analytical data for all new compounds. This material is available free of charge via the Internet at http://pubs.acs.org.